Anatomical Analysis of an Aye-Aye Brain (*Daubentonia madagascariensis*, Primates: Prosimii) Combining Histology, Structural Magnetic Resonance Imaging, and Diffusion-Tensor Imaging

JASON A. KAUFMAN,[1] ERIC T. AHRENS,[2] DAVID H. LAIDLAW,[3] SONG ZHANG,[3] AND JOHN M. ALLMAN[1]*

[1]Division of Biology, California Institute of Technology, Pasadena, California
[2]Department of Biological Sciences and the Pittsburgh NMR Center for Biomedical Research, Carnegie Mellon University, Pittsburgh, Pennsylvania
[3]Department of Computer Science, Brown University, Providence, Rhode Island

ABSTRACT

This report presents initial results of a multimodal analysis of tissue volume and microstructure in the brain of an aye-aye (*Daubentonia madagascariensis*). The left hemisphere of an aye-aye brain was scanned using T2-weighted structural magnetic resonance imaging (MRI) and diffusion-tensor imaging (DTI) prior to histological processing and staining for Nissl substance and myelinated fibers. The objectives of the experiment were to estimate the volume of gross brain regions for comparison with published data on other prosimians and to validate DTI data on fiber anisotropy with histological measurements of fiber spread. Measurements of brain structure volumes in the specimen are consistent with those reported in the literature: the aye-aye has a very large brain for its body size, a reduced volume of visual structures (V1 and LGN), and an increased volume of the olfactory lobe. This trade-off between visual and olfactory reliance is likely a reflection of the nocturnal extractive foraging behavior practiced by *Daubentonia*. Additionally, frontal cortex volume is large in the aye-aye, a feature that may also be related to its complex foraging behavior and sensorimotor demands. Analysis of DTI data in the anterior cingulum bundle demonstrates a strong correlation between fiber spread as measured from histological sections and fiber spread as measured from DTI. These results represent the first quantitative comparison of DTI data and fiber-stained histology in the brain.

Key words: aye-aye; *Daubentonia*; brain volume; histology; magnetic resonance imaging; diffusion-tensor imaging

The aye-aye (*Daubentonia madagascariensis*) is a remarkable primate in many respects. A Malagasy prosimian, *Daubentonia* is the largest nocturnal primate and the most highly encephalized of the Strepsirhini (Stephan et al., 1981, 1988). Its ecological niche is distinct from any other primate; though they consume a wide range of gums, nectars, and insects, *Daubentonia* is a specialist in extractive foraging, subsisting largely on insect larvae that lie burrowed beneath tree bark (Ganzhorn and Rabesoa, 1986; Sterling, 1993; Sterling et al., 1994). The aye-aye has several morphological features that are clearly adaptive for extractive foraging: large mobile pinnae, perpetually growing incisors for gnawing wood, and an elongated third digit that functions as a probe for extracting larvae from cavities (Petter et al., 1977; Tattersall, 1982). The modified finger is also used to tap the wood surface, apparently to generate acoustical cues that are used for prey capture (Milliken et al., 1991; Erickson, 1994).

*Correspondence to: John M. Allman, Division of Biology, California Institute of Technology, MC 216-76, Pasadena, CA 91125. Fax: 626-449-0679. E-mail: cebus@caltech.edu

Received 16 August 2005; Accepted 17 August 2005
DOI 10.1002/ar.a.20264
Published online 7 October 2005 in Wiley InterScience (www.interscience.wiley.com).

Little is known about the brain of *Daubentonia*, but there is reason to believe that its large relative brain size may be related to its distinct ecological niche. Gibson (1986) argued that the four most-encephalized primate species (*Homo*, *Pan*, *Cebus*, and *Daubentonia*) all share omnivorous diets and are all adapted for exploiting cryptic, defended resources. Gibson (1986) and Sterling (1994) have suggested that the high degree of encephalization seen in *Daubentonia* could be related to its complex foraging behaviors and associated sensorimotor activities. Recently, Bush and Allman (2004) examined frontal cortex volume in a variety of primates and carnivores, including the right hemisphere of the *Daubentonia* individual used in this study, and found that *Daubentonia* has a large frontal cortex for its brain size.

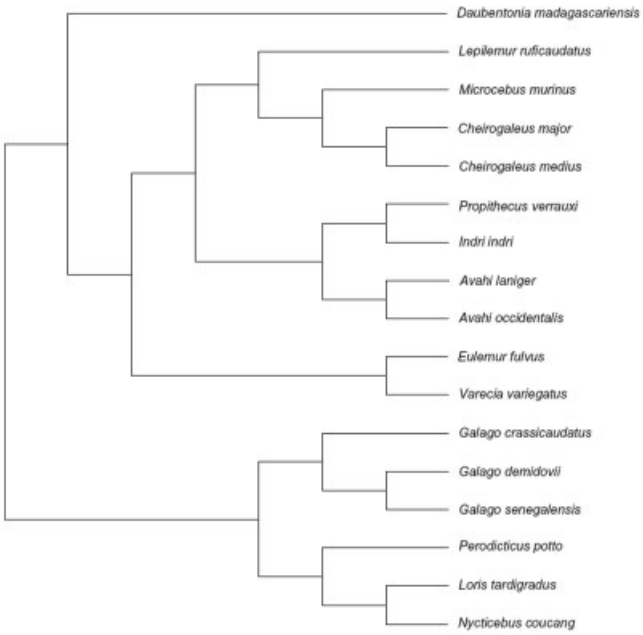

Fig. 1. Prosimian phylogeny used for independent contrast analysis. Adapted from Yoder (1994), Yoder and Yang (2004), and Karnath et al. (2005).

There is also a possibility that *Daubentonia*'s large brain size is in part a consequence of a secondary reduction in body mass from a larger-bodied ancestor (Lamberton, 1934; Bauchot and Stephan, 1969; Frahm et al., 1982). The only other known species of Daubentoniidae is the subfossil *Daubentonia robusta* (Lamberton, 1934), a member of a diverse array of recently extinct giant lemurs (Godfrey and Jungers, 2003) that is estimated to have been approximately 13.5 kg—three to five times the size of the extant *D. madagascariensis* (Simons, 1994).

We recently had the opportunity to begin analyzing a fixed, intact aye-aye brain. Our goal has been to apply a multimodal approach to this unique brain specimen, including high-resolution conventional magnetic resonance imaging (MRI), diffusion-tensor imaging (DTI), and histological staining for Nissl and myelinated fibers. DTI is a variant of MRI that is used to measure the orientation and coherence of white matter fiber tracts in vivo or in isolated tissue specimens (Basser et al., 1994b). Our initial analy-

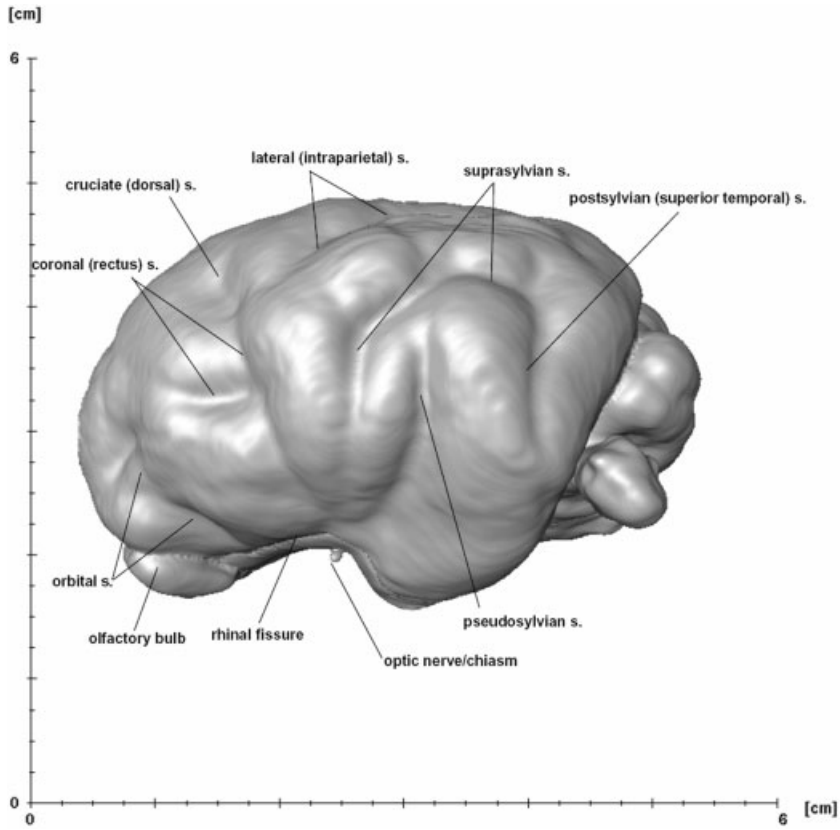

Fig. 2. Lateral view of the reconstructed left hemisphere of the aye-aye brain. Sulcal terminology from Connolly (1950). Names in parentheses refer to conventional terminology used for primates.

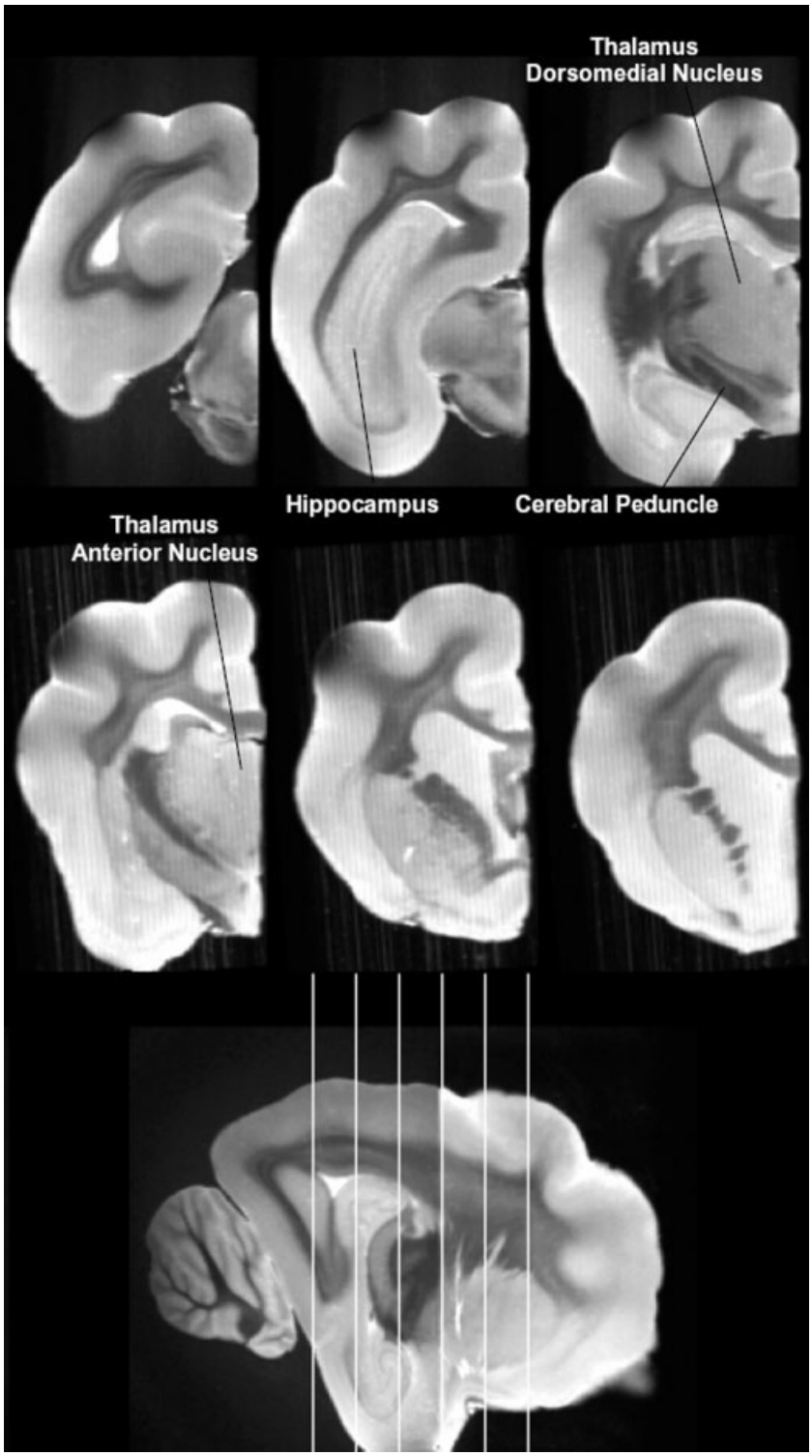

Fig. 3. Coronal sections through the T2-weighted MRI scan of the *Daubentonia* left hemisphere.

sis focuses first on digital reconstruction of the MR-imaged left hemisphere and on volumetric estimates of gross brain subdivisions for comparison with the aye-aye data point of Stephan et al. (1981). We begin by illustrating some features of the cortical morphology and then present some preliminary results on *Daubentonia* brain volume in comparison with 16 other prosimian species represented in the data set of Stephan et al. (1981). Using both conventional least-squares regression and phylogenetically independent contrasts, we analyze the allometric relationships of individual brain components across prosimians. Since we do not have body mass data for our *Daubentonia*

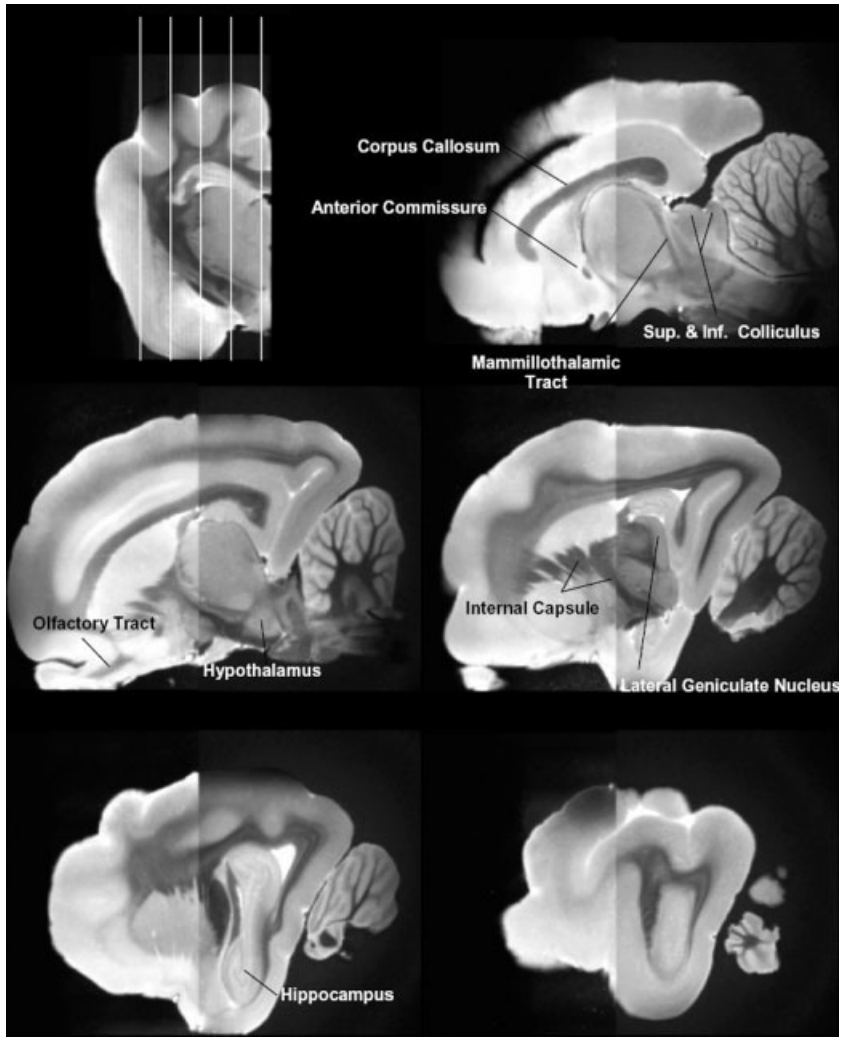

Fig. 4. Sagittal sections through the T2-weighted MRI scan of the *Daubentonia* left hemisphere.

individual, we model our regression using structure volume as the dependent variable and whole brain volume minus structure volume (i.e., the rest of the brain) as the independent variable (Barton, 1999).

The DTI technique assays the magnitude and spatial directionality of Brownian water diffusion in tissue (Le Bihan and Breton, 1985; Le Bihan et al., 2001). Water that diffuses more readily in some directions compared to others due to features in the tissue microstructure is said to have anisotropic diffusion. In the brain, water diffuses more readily along axon tracts compared to transverse directions (Beaulieu and Allen, 1994a, 1994b). DTI can be used to measure this anisotropy, which in turn can be used to visualize the fiber's trajectory and coherence (Le Bihan et al., 2001). The magnitude and direction of the water diffusion is modeled by a second-order diffusion-tensor at each point in a volume image, and the relative coherence or uniformity of spatial diffusion can be quantified using the fractional anisotropy (FA), a ratio of the eigenvalues of the tensor. Fractional anisotropy ranges from 0 (isotropic diffusion) to 1 (highly anisotropic diffusion). Nominally, the value of FA is $\simeq 0$ in gray matter, > 0 in white matter, and approaches unity in large coherent tracts.

DTI and its associated tractography techniques have been successfully applied in a variety of clinical and research settings (reviewed by Le Bihan et al., 2001; Michael, 2002; Moseley et al., 2002; Neil et al., 2002; Ramnani et al., 2004; Sundgren et al., 2004), but the relationship between DTI data and brain microstructure is not fully understood. In isolated rabbit myocardium, DTI data on muscle fiber orientation have been shown to correlate well with orientation measurements performed directly on histological preparations subsequent to scanning (Hsu et al., 1998; Scollan et al., 1998; Holmes et al., 2000). Here we apply a similar analysis by estimating a histological analogue of FA, which we defined as the variance of axon orientations within a microscopic volume. We calculated axon orientation distributions from a series of sites within the anterior cingulum bundle using stereologic microscopy and compared these values with fiber spread data as measured by the DTI-derived FA parameter. We chose the cingulum bundle for this analysis since the hemisphere was sectioned in the sagittal plane and the fibers of the cingulum bundle run primarily within the plane of sectioning.

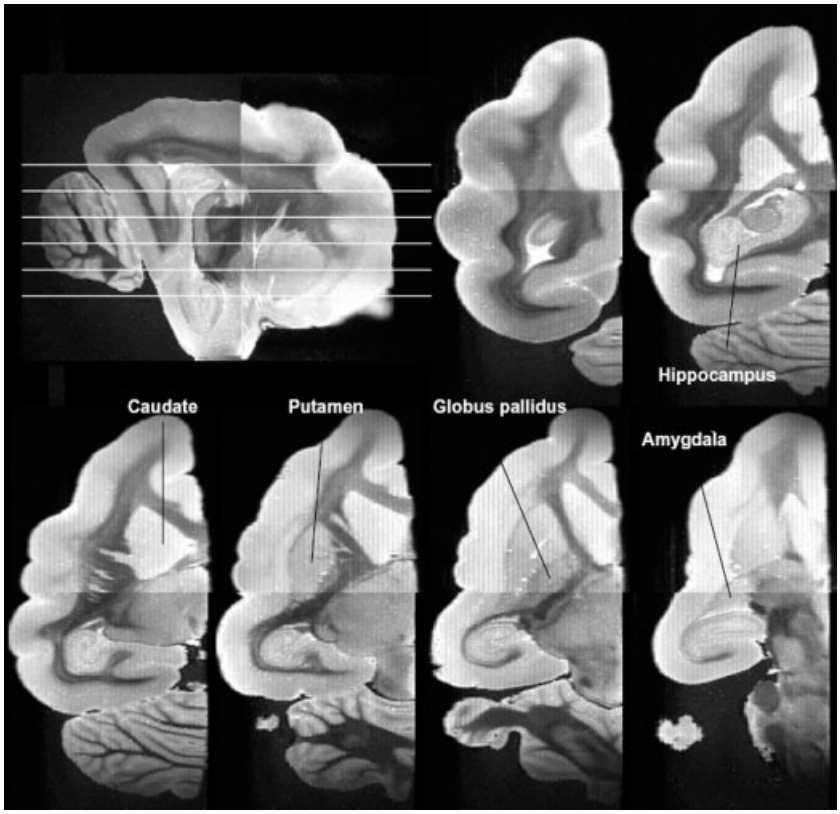

Fig. 5. Axial sections through the T2-weighted MRI scan of the *Daubentonia* left hemisphere.

MATERIALS AND METHODS

The aye-aye died of natural causes at the Duke University Primate Center and was immediately frozen at −80°C. Later it was thawed and the brain removed and fixed in 4% paraformaldehyde. Before imaging, the left hemisphere was rinsed in PBS, immersed in Fluorinert (Sigma-Aldrich, Inc.), and positioned in a 35 mm inner diameter birdcage MRI coil. Images were acquired using an 11.7 T, 89 mm vertical-bore Bruker microimaging system. The three-dimensional (3D) DTI data were built from three overlapping packets of 32 contiguous slices acquired using a pulsed-gradient spin-echo protocol (Basser et al., 1994a). Each slice packet was translated along the slice direction by one-third of the slice thickness. Postprocessing interleaved the slices for a final isotropic voxel size of approximately 70 μm. A total of 29 volumetric images were used in fitting the diffusion-tensors. The diffusion gradients were applied along seven different directions, and four values of b-matrix magnitude were used along each direction (maximum b ≃ 1,500 mm^2/sec). Images were acquired with TR/TE = 2000/19 msec and 512 × 256 × 96 image points. The tensors were fit using a laboratory-written nonlinear fitting algorithm (Zhang et al., 2003). The anatomical T2 images were a by-product of the DTI fitting process. The brain hemisphere was scanned in two volumes, one for the rostral portion and a second for the caudal portion of the brain, and then they were digitally merged.

We also prepared a complete histological series from the left hemisphere. The hemisphere was immersion-fixed in formalin and embedded in celloidin. We have found that celloidin provides better staining results, with less tissue shrinkage, than other embedding media. The hemisphere was sectioned in the parasagittal plane at a thickness of 50 μm, and the complete series was alternately stained for Nissl substance (thionin stain) and for myelinated axons (Gallyas, 1979). To help ensure accurate registration of the MRI with histological sections, the cut face of the celloidin block was photographed with a digital camera mounted in a stationary position above the microtome. The mounted sections were digitized with a flatbed scanner, and each image was registered with its corresponding photograph of the cut face. A 3D rendering of the hemisphere, assembled from the registered images, was used to select sites on the histological sections that corresponded to regions that could be identified on the MRI.

TABLE 1. Size of the *Daubentonia* brain and its components as calculated in this study compared with the values calculated by Stephan et al. (1981)

	Present Study	Stephan et al., 1981
Whole Brain (mg)	38130	45150
Neocortex (mm^3)	22029	22127
Cerebellum (mm^3)	4602	6461
Thalamus (mm^3)	1512	-
Hippocampus (mm^3)	1561	1776
Striatum (mm^3)	2450	2765
Visual Striate Cortex (mm^3)	1028	1355
Lateral Geniculate Nucleus (mm^3)	48	59
Neocortical White (mm^3)	4347	5053

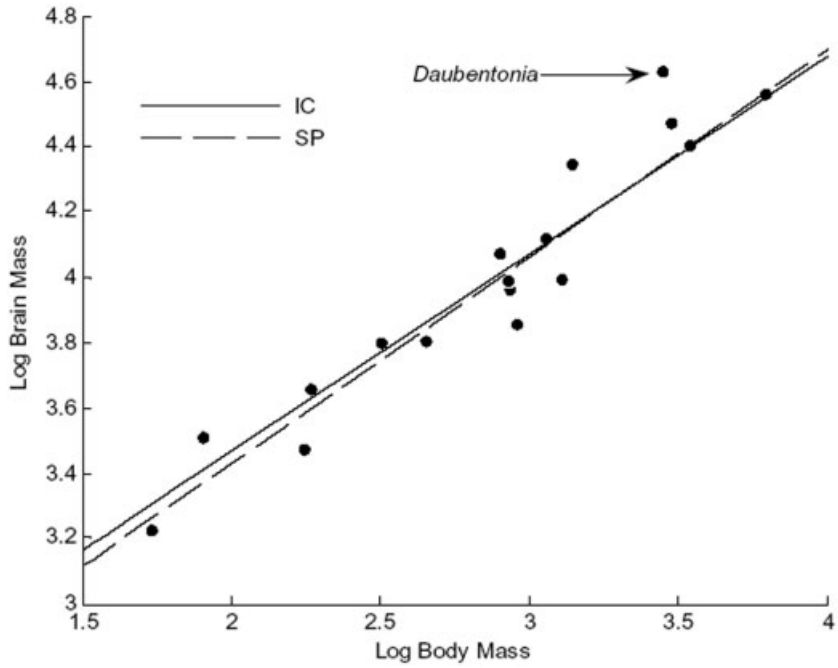

Fig. 6. Body mass regressed on brain mass in prosimians. IC, independent contrasts; SP, star phylogeny.

TABLE 2. Regression statistics for allometric analyses among prosimians, computed without *Daubentonia*

				95% Confidence Intervals	
Structure (Fig.)		R^2	Slope	Lower Bound	Upper Bound
Brain: Body (Fig 6)	IC	0.93	0.61	0.52	0.70
	SP	0.93	0.63	0.53	0.73
Cerebellum (Fig. 7a)	IC	0.98	1.02	0.95	1.10
	SP	0.98	1.02	0.94	1.10
Telencephalon (Fig. 7b)	IC	0.98	1.03	0.95	1.11
	SP	0.99	1.03	0.96	1.11
Diencephalon (Fig. 7c)	IC	0.99	1.00	0.93	1.06
	SP	0.99	1.02	0.97	1.06
Mesencephalon (Fig. 7d)	IC	0.95	0.79	0.69	0.90
	SP	0.98	0.79	0.73	0.86
Neocortex (Fig. 7e)	IC	0.97	1.08	0.97	1.19
	SP	0.98	1.14	1.05	1.23
Visual Striate Cx (Fig. 7f)	IC	0.89	0.83	0.66	0.98
	SP	0.94	0.87	0.74	0.10
Lateral Geniculate N. (Fig 7g)	IC	0.90	0.79	0.64	0.94
	SP	0.94	0.82	0.71	0.94
Olfactory Bulb (Fig. 7h)	IC	0.70	0.67	0.42	0.92
	SP	0.58	0.49	0.25	0.73

IC, Independent Contrasts Regression; SP, Star Phylogeny (Ordinary Least Squares)

Volumetric measurements were calculated by manually segmenting the T2-weighted MRI scans or, in the case of visual striate cortex, a combination of Nissl and fiber stains using the software package Amira (TGS, San Diego, CA). Allometric regressions were calculated using conventional least-squares regression (hereafter termed "star phylogeny") as well as phylogenetically independent contrasts. For *Daubentonia*, data points represent the mean of our individual and Stephan's individual, and *Daubentonia* was excluded from the sample when calculating regression equations. For independent contrast regression, the assumed prosimian branching order (Fig. 1) was adapted from previous studies (Yoder, 1994; Yoder and Yang, 2004; Karanth et al., 2005). Independent contrast regression statistics were calculated using the software package PDAP (Garland et al., 1999; Garland and Ives, 2000). To satisfy the statistical requirements of independent contrast regression, the branch lengths were transformed using Pagel's (1992) method, which sets all branch lengths equal to 1 with the condition that tips are contemporaneous. For graphical illustration, we use the method of Garland and Ives (2000) to map the independent contrast regression line back into raw data space.

Using the Gallyas stain, it was possible to trace individual axons at high magnification and fiber bundles at low magnification. Fiber tracings were performed at 14 sites

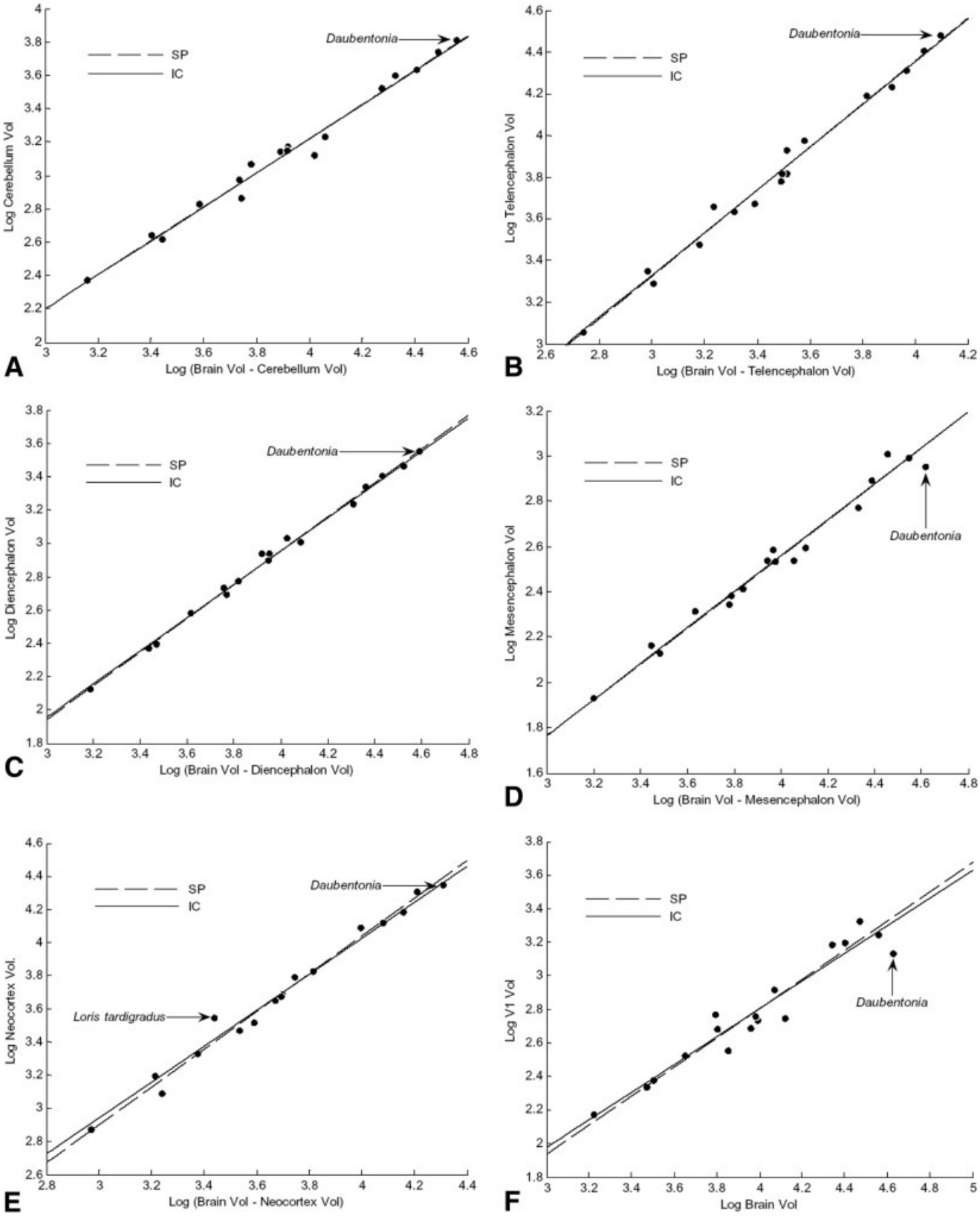

Fig. 7. Scatterplots of brain structure volume compared to the volume of the rest of the brain in (**A**) cerebellum, (**B**) telencephalon, (**C**) diencephalon, (**D**) mesencephalon, (**E**) neocortex, (**F**) visual striate cortex, (**G**) lateral geniculate nucleus, and (**H**) olfactory bulb.

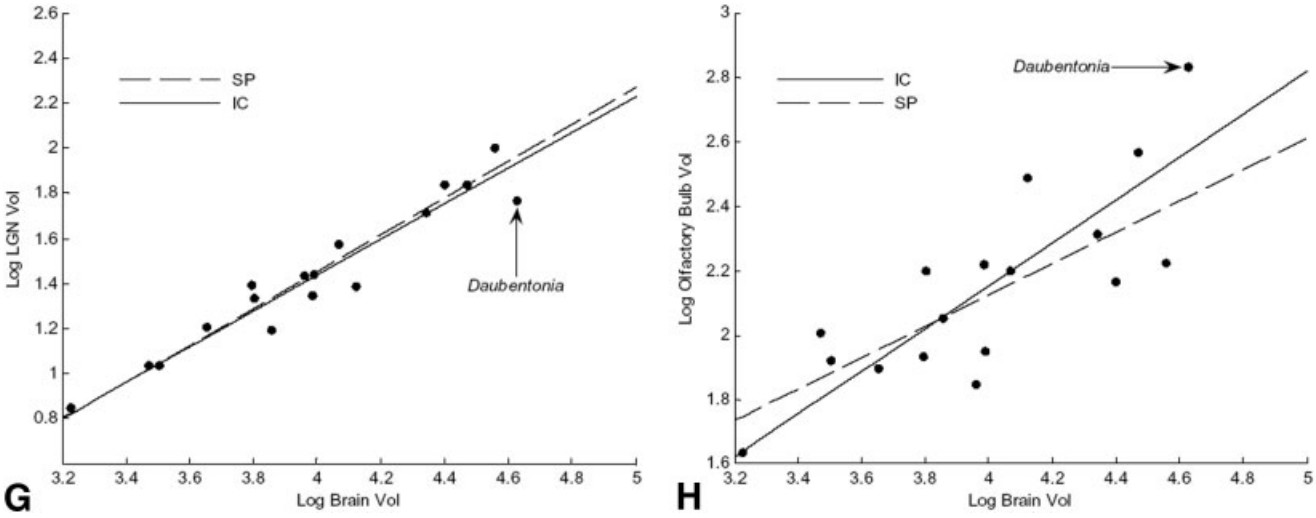

Figure 7 (Continued)

along the anterior cingulum bundle using a Reichert-Jung microscope and Neurolucida software (MicroBrightField, Wiliston, VT). We chose to focus initially on the cingulum bundle since these fibers run primarily in the plane of sectioning. Tracings from each sample site were analyzed using Neurolucida's directional statistics package to calculate the distribution of fiber orientations. As a histological analogue of FA, we computed the standard deviation of this orientation distribution within each sample site. Tests of intrarater repeatability demonstrated good precision. At low magnification (where measurement error is greatest), repeated estimates of fiber orientation yielded a coefficient of variation of 2.8% (n = 6), with an average difference in mean fiber orientation of 8°.

RESULTS

Volumetry

Figure 2 illustrates a 3D rendering of the aye-aye left hemisphere as reconstructed from the structural MRI scan. The surface morphology appears quite similar to that of a carnivore brain, with certain features not found in any other primate. Rather than exhibiting a classical primate Sylvian fissure, the pseudosylvian sulcus in *Daubentonia* is surrounded by a concentric arc formed by the suprasylvian and postsylvian sulci. Connolly (1950: p. 9) notes that "the cortex between the anterior portion of the suprasylvian and the pseudosylvian becomes operculated in some of the lower mammals and in all primates with the exception of the aye-aye, so that the suprasylvian becomes engulfed and appears superficially to merge with the pseudosylvian."

The coronal sulcus is sharply angled, with a posterior portion that is confluent with a pronounced cruciate (dorsal) sulcus. Ziehen (1896) suggested that, in lemurs, the dorsal sulcus and the angled caudal portion of the coronal sulcus are homologous to the central sulcus of higher primates.

The orbital sulcus in *Daubentonia* appears quite pronounced compared with other lemurs. Beginning from the anterior rhinal fissure, the orbital sulcus extends upward and bifurcates rostrally, resembling the morphology of a carnivore brain.

Representative orthogonal slices from T2-weighted MRI are presented in Figures 3–5. The fixed brain yielded high contrast between gray and white matter structures. The results of our volumetric estimates, along with the corresponding values from Stephan et al. (1981, 1988), are presented in Table 1. Our aye-aye brain is smaller than that of Stephan et al. (1981, 1988); we calculated a total brain weight of 38.13 g, compared to theirs of 45.15 g. Qualitatively, however, there is good correspondence between our data and theirs.

Figure 6 illustrates the results of allometric regressions for body mass on brain weight among prosimians. Since we do not have a body mass measurement for our specimen, this regression includes only the *Daubentonia* specimen from the data set of Stephan et al. (1981, 1988). Regression statistics and confidence intervals are provided in Table 2. As others have noted, the high degree of encephalization in *Daubentonia* is clearly evident. However, most individual brain components appear to scale proportionally in the aye-aye when compared with the volume of the rest of the brain (Fig. 7). The volumes of the neocortex, cerebellum, telencephalon, and diencephalon are all consistent with general prosimian scaling trends. The mesencephalon appears slightly reduced in size (Fig. 7D). The aye-aye also exhibits a markedly reduced visual system, as is evident from the comparatively small volumes of the lateral geniculate nucleus and visual striate cortex. In comparison, the olfactory bulb appears to be greatly enlarged in *Daubentonia*.

Diffusion-Tensor Imaging

Figure 8 illustrates the results of diffusion-tensor imaging. In Figure 8A, we show a photomicrograph of the callosal genu and anterior cingulum bundle (outlined) stained for myelin. Figure 8B shows DTI data in the same region; these data were rendered in such a way that the diagonal elements of the effective diffusion-tensor are displayed as a single composite image, where each color

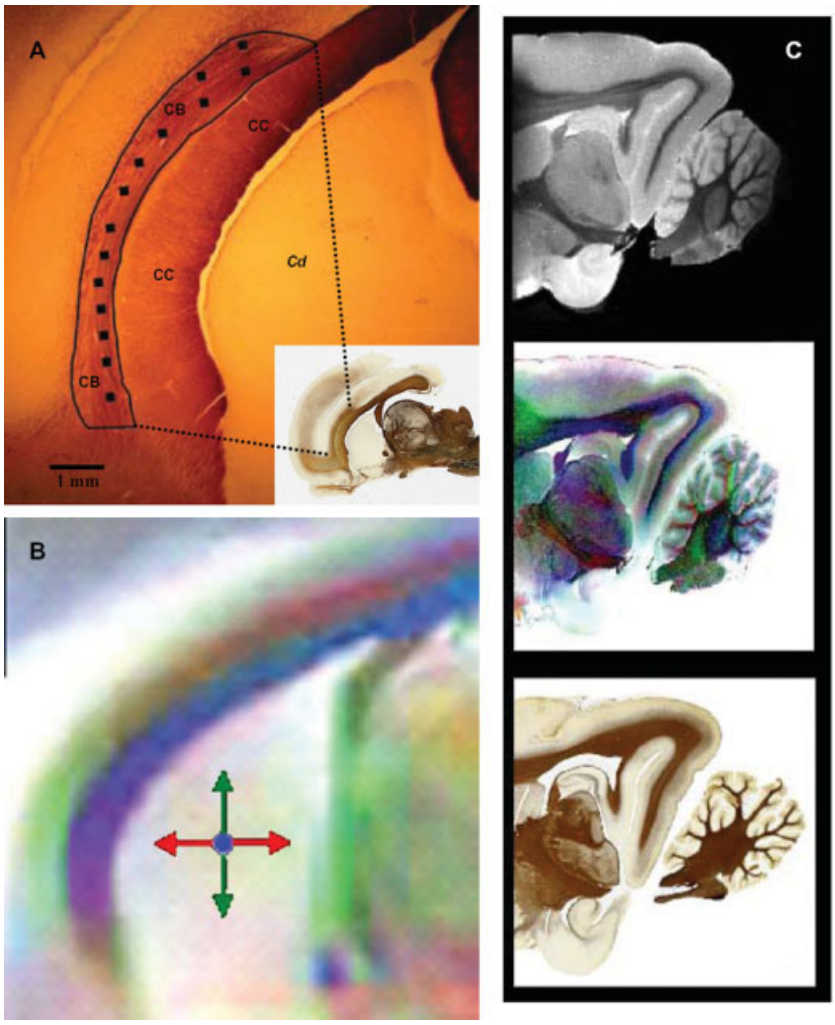

Fig. 8. White matter visualization using histology and magnetic resonance imaging. **A:** Gallyas fiber stain of the callosal genu and anterior cingulum bundle. CC, corpus callosum; CB, cingulum bundle; Cd, caudate nucleus. **B:** Diffusion-tensor image of the callosal genu and anterior cingulum in which the principal direction of diffusion is coded in pseudocolor format. Fiber direction is indicated by hue (red, anterior-posterior; green, superior-inferior; blue, medial-lateral). **C:** Comparison of imaging modalities. Top: T2-weighted MRI. Middle: Color-coded diffusion-tensor MRI. Bottom: Gallyas fiber stain.

channel (red, green, blue) is assigned to a diagonal tensor element. Regions showing predominantly a single color represent fiber tracts with a high degree of coherence along a color-coded direction. Gray matter regions appear gray due to the diffusion isotropy in this material. The corpus callosum stands out as a dominant blue tract of fibers running orthogonal to the image plane. Green tracts, such as the fornix, run primarily in the superior-inferior direction, while red areas contain tracts oriented anteroposteriorly. The cingulum bundle gradually changes from green to red as the fibers progress caudally over the corpus callosum. Figure 8C illustrates the excellent correspondence between three visualizations of the caudal portion of the brain.

Comparisons of selected slices from the 3D DTI data set and the fiber-stained histological tracings indicate good correspondence between the DTI-derived FA parameter and the fiber spread as measured from the histological sections. Figure 9A indicates the location of various tracing sites contained within the region outlined in Figure 8A. Two tracing sites are highlighted, exhibiting differing fiber coherence. When the histological fiber spread is plotted against FA (Fig. 10), the results confirm that DTI provides a quantitative assay of white matter structure; areas with high FA have smaller orientation distributions compared with areas of low FA ($R^2 = 0.56$).

DISCUSSION

In our analysis of *Daubentonia*, estimates of brain structure volumes are consistent with values reported by Stephan et al. (1981). In their allometric analysis, Stephan et al. (1981) found that nearly all brain structures in the aye-aye exhibit progression indexes higher than in any other prosimian. However, it is important to note that Stephan et al. (1981) calculated their allometric prediction equations using basal insectivores as a reference, while we have restricted our analysis to prosimians only. We found that while *Daubentonia* does have a relatively large brain for its body mass among prosimians, its neocortex is no larger than would be expected considering the size of the rest of the brain. There is evidence of a reduction in the volume of the midbrain, but the other major brain components do not show any marked deviation from the prosimian trend.

We hasten to emphasize that our volumetric analysis is much more conservative than one in which brain structures are analyzed in relation to body mass. With the exception of V1, LGN, and the olfactory bulb, each major

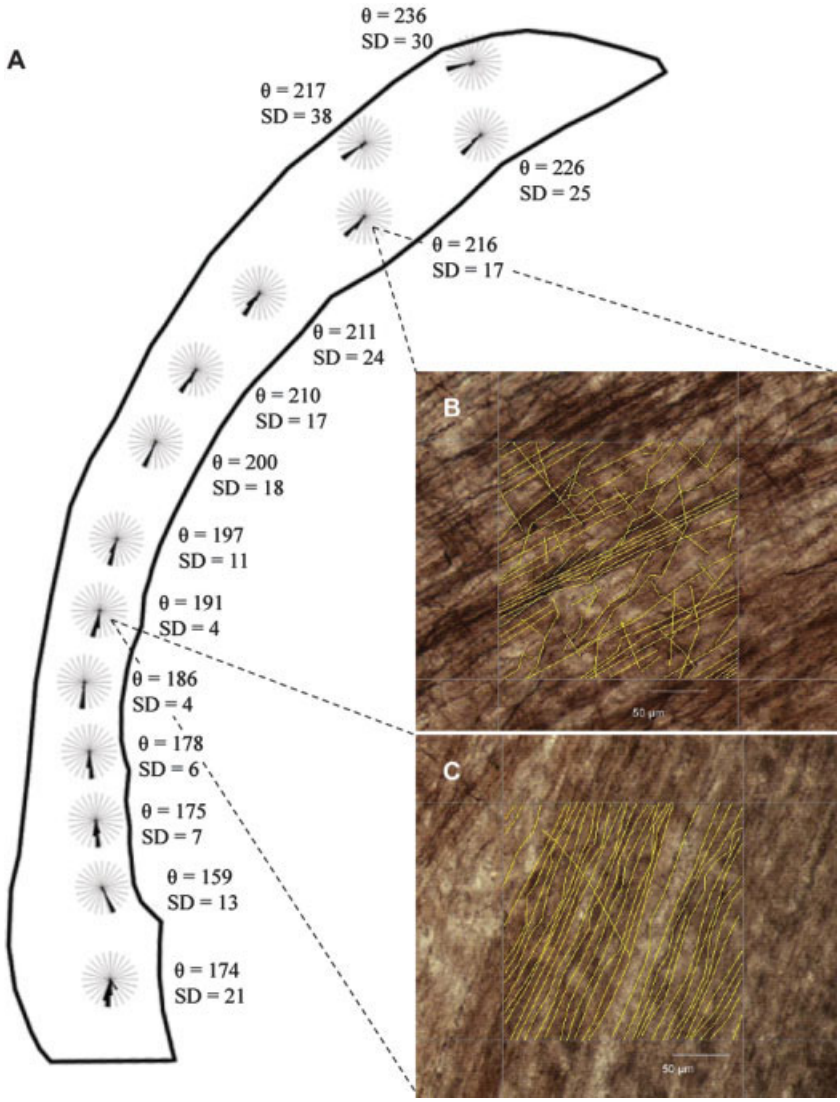

Fig. 9. Fiber tracings from a sequence of sites in the anterior cingulum bundle. **A:** Polar histograms centered on each sample site depict fiber orientation. **B** and **C:** Examples of fiber tracings from two sites with differing degrees of fiber coherence.

brain component examined here constitutes a significant proportion of overall brain size, and therefore the two variables are highly intercorrelated. At the same time, there are strong indications of a trade-off in visual and olfactory reliance in the aye-aye that is quite different from the typical primate pattern of large visual structures and small olfactory structures (Allman, 2000). The relative volumes of sensory structures in *Daubentonia* are consistent with its ecological niche as a nocturnal extractive forager: the volumes of lateral geniculate nucleus and visual striate cortex are reduced, while the olfactory bulb appears greatly enlarged. We note also that the inferior colliculus appears quite large in the aye-aye (Fig. 4), and that this feature probably highlights the auditory demands of percussive foraging.

Recently, Bush and Allman (2004) examined frontal cortex volume in a variety of primates and carnivores, including the right hemisphere of the *Daubentonia* individual used in this study, and found that *Daubentonia* has a large frontal cortex for its brain size. Figure 11 illustrates a plot of their data for strepsirhines only. Since we have an a priori hypothesis about frontal enlargement in the aye-aye brain, the regression equations were calculated without the aye-aye data point. Indeed, the *Daubentonia* residual is comparatively large: the aye-aye appears to have a large frontal cortex for its brain size. This is a significant finding, especially in light of the high level of sensorimotor intelligence thought to be associated with the complex foraging behavior observed in *Daubentonia* (Parker and Gibson, 1977; Gibson, 1986). An enlarged frontal cortex in the aye-aye could also be associated with the need to integrate a large amount of sensory information during foraging. Sterling (1993) even reported observing object manipulation in wild aye-ayes in the form of manipulating and repositioning lianas to gain access to food, though such behavior could not be reliably reproduced in the laboratory (Sterling and Povinelli, 1999).

The fact that the external morphology of the aye-aye brain appears similar to that of a carnivore further raises the possibility of evolutionary divergence from the typical primate pattern toward a carnivore configuration. A secondary reduction of visual structures, with concomitant

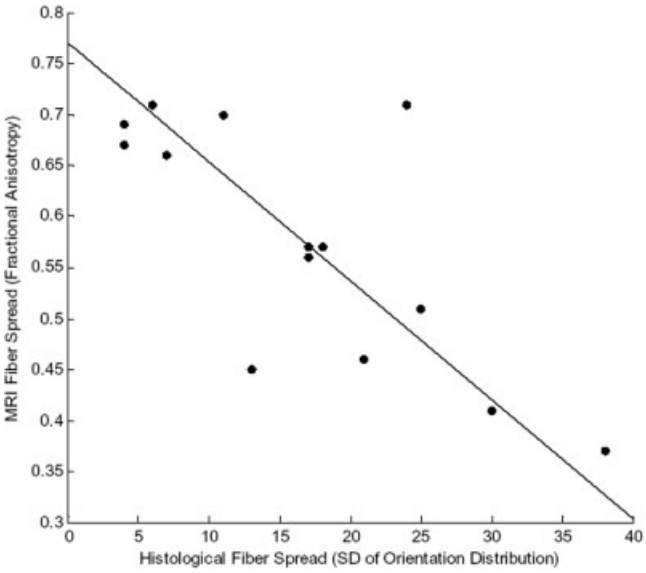

Fig. 10. Scatterplot of fiber spread as measured from histological tracings versus fiber spread as measured from DTI. The line represents the reduced major-axis best-fit line ($R^2 = 0.56$).

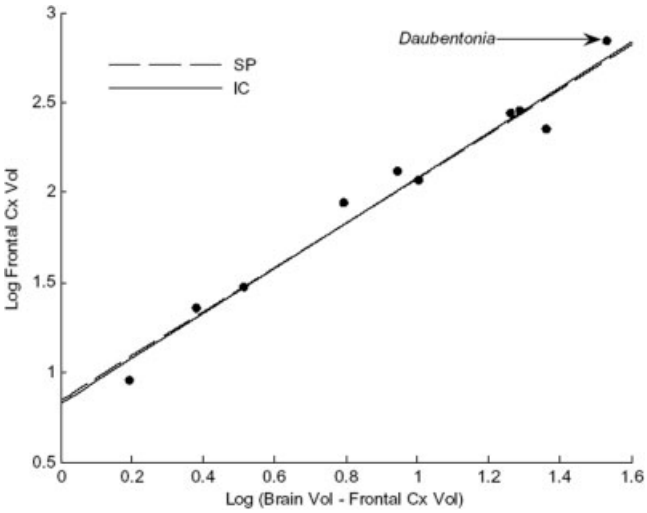

Fig. 11. Scatterplot of frontal cortex volume versus volume of the rest of the brain in prosimians. Data from Bush and Allman (2004).

expansion of auditory and olfactory structures, may contribute to the atypical morphology illustrated here. It is also possible that craniodental features, such as the continually growing incisors, have an effect on brain shape in the aye-aye.

Finally, the results of our DTI and histological analysis show a good correlation between white matter coherence data obtained from DTI and histology. We found a significant correlation between FA and histological fiber spread (Pearson correlation coefficient = −0.75), confirming that DTI can assay meaningful white matter morphology on the microscopic scale. Previously, several groups performed direct comparisons of muscle fiber orientation using DTI and histology in rabbit (Scollan et al., 1998; Holmes et al., 2000) and canine (Hsu et al., 1998) myocardial tissue. They found excellent agreement between the two methods, with correlation coefficients between 0.86 and 0.95 depending on the DTI pulse sequence. It is important to note that these groups measured fiber orientation as derived from the principal eigenvector, while we computed the fiber spread via FA, which is derived from the full set of directional vectors. We therefore expect our correlation to be lower since the computation of FA entails greater error variance. In this light, the high correlation found here (~ 0.75) strongly substantiates the use of DTI in studies of white matter morphology across species, in addition to the important DTI studies on development and pathology in the human brain.

ACKNOWLEDGMENTS

The authors thank the Duke University Primate Center for providing the aye-aye brain and Virginie Goubert for expert assistance with histological preparation. Supported by the David and Lucile Packard Foundation (to J.M.A.), the Gordon and Betty Moore Foundation (to J.M.A.), the National Science Foundation (CCR-0086065 to D.H.L.), and the National Institutes of Health (RO1-EB003453, P41-EB001977, and P50-ES049617 to E.T.A.).

LITERATURE CITED

Allman JM. 2000. Evolving brains. New York: W.H. Freeman.

Barton RA. 1999. The evolutionary ecology of the primate brain. In: Lee P, editor. Comparative primate socioecology. Cambridge: Cambridge University Press. p 167–194.

Basser PJ, Mattiello J, Lebihan D. 1994a. Estimation of the effective self-diffusion tensor from the NMR spin echo. J Magn Reson Ser B 103:247.

Basser PJ, Mattiello JJ, LeBihan DD. 1994b. MR diffusion tensor spectroscopy and imaging. Biophys J 66:259–267.

Bauchot R, Stephan H. 1969. Encéphalisation et niveau évolutif chez les simiens. Mammalia 33:225–275.

Beaulieu C, Allen PS. 1994a. Determinants of anisotropic water diffusion in nerves. Magn Reson Med 31:394–400.

Beaulieu C, Allen PS. 1994b. Water diffusion in the giant axon of the squid: implications for diffusion-weighted MRI of the nervous system. Magn Reson Med 32:579–583.

Bush EC, Allman JM. 2004. The scaling of frontal cortex in primates and carnivores. Proc Natl Acad Sci USA 101:3962–3966.

Connolly CJ. 1950. External morphology of the primate brain. Springfield: Charles C. Thomas.

Erickson CJ. 1994. Tap-scanning and extractive foraging in aye-ayes, *Daubentonia madagascariensis*. Folia Primatol (Basel) 62:125–135.

Frahm HD, Stephan H, Stephan M. 1982. Comparison of brain structure volumes in Insectivora and Primates: I, neocortex. J Hirnforsch 23:375–389.

Gallyas F. 1979. Silver staining of myelin by means of physical development. Neurol Res 1:203–209.

Ganzhorn JU, Rabesoa J. 1986. The aye-aye (*Daubentonia madagascariensis*) found in the eastern rainforest of Madagascar. Folia Primatol (Basel) 46:125–126.

Garland T Jr, Midford PE, Ives AR. 1999. An introduction to phylogenetically based statistical methods, with a new method for confidence intervals on ancestral states. Am Zool 39:374–388.

Garland T Jr, Ives AR. 2000. Using the past to predict the present: Confidence intervals for regression equations in phylogenetic comparative methods. Am Nat 155:346–364.

Gibson KR. 1986. Cognition, brain size and the extraction of embedded food resources. In: Else JG, editor. Primate evolution. New York: Cambridge University Press. p 93–103.

Godfrey LR, Jungers WL. 2003. The extinct sloth lemurs of Madagascar. Evol Anthropol 12:252–263.

Holmes AA, Scollan DF, Winslow RL. 2000. Direct histological validation of diffusion tensor MRI in formaldehyde-fixed myocardium. Magn Reson Med 44:157–161.

Hsu EW, Muzikant AL, Matulevicius SA, Penland RC, Henriquez CS. 1998. Magnetic resonance myocardial fiber-orientation mapping with direct histological correlation. Am J Physiol Heart Circ Physiol 274:H1627–H1634.

Karanth KP, Delefosse T, Rakotosamimanana B, Parsons TJ, Yoder AD. 2005. Ancient DNA from giant extinct lemurs confirms single origin of Malagasy primates. Proc Natl Acad Sci USA 102:5090–5095.

Lamberton C. 1934. Contribution à la connaissance de la faune subfossile de Madagascar. Mem Acad Malagache 17:40–46.

Le Bihan D, Breton E. 1985. Imagerie de diffusion in-vivo par résonance magnétique nucléaire. CR Acad Sci (Paris) 301:1109–1112.

Le Bihan D, Mangin JF, Poupon C, Clark CA, Pappata S, Molko N, Chabriat H. 2001. Diffusion tensor imaging: concepts and applications. J Magn Reson Imaging 13:534–546.

Michael M. 2002. Diffusion tensor imaging and aging: a review. NMR Biomed 15:553–560.

Milliken GW, Ward JP, Erickson CJ. 1991. Independent digit control in foraging by the aye-aye (*Daubentonia madagascariensis*). Folia Primatol (Basel) 56:219–224.

Moseley M, Bammer R, Illes J. 2002. Diffusion-tensor imaging of cognitive performance. Brain Cogn 50:396.

Neil J, Miller J, Mukherjee P, Hüppi PS. 2002. Diffusion tensor imaging of normal and injured developing human brain: a technical review. NMR Biomed 15:543–552.

Pagel MD. 1992. A method for the analysis of comparative data. J Theor Biol 156:431–442.

Parker ST, Gibson KR. 1977. Object manipulation, tool use and sensorimotor intelligence as feeding adaptations in cebus monkeys and great apes. J Hum Evol 6:623–641.

Petter J-J, Albignac R, Rumpler Y. 1977. Mammifères Lémuriens (Primates Prosimiens). Paris: ORSTOM and CNRS.

Ramnani N, Behrens TEJ, Penny W, Matthews PM. 2004. New approaches for exploring anatomical and functional connectivity in the human brain. Biol Psychiatry 56:613.

Scollan DF, Holmes A, Winslow R, Forder J. 1998. Histological validation of myocardial microstructure obtained from diffusion tensor magnetic resonance imaging. Am J Physiol 275:H2308–H2318.

Simons EL. 1994. The giant aye-aye Daubentonia robusta. Folia Primatol (Basel) 62:14–21.

Stephan H, Frahm H, Baron G. 1981. New and revised data on volumes of brain structures in insectivores and primates. Folia Primatol (Basel) 35:1–29.

Stephan H, Baron G, Frahm H. 1988. Comparative size of brains and brain components. In: Steklis HD, Erwin J, editors. Comparative primate biology, vol. 4, neurosciences. New York: Alan R. Liss. p 1–38.

Sterling EJ. 1993. Behavioral ecology of the aye-aye (*Daubentonia madagascariensis*) on nosy mangabe, Madagascar. PhD thesis. New Haven, CT: Yale University.

Sterling EJ. 1994. Aye-ayes: specialists on structurally defended resources. Folia Primatol (Basel) 62:142–154.

Sterling EJ, Dierenfeld ES, Ashbourne CJ, Feistner AT. 1994. Dietary intake, food composition and nutrient intake in wild and captive populations of *Daubentonia madagascariensis*. Folia Primatol (Basel) 62:115–124.

Sterling EJ, Povinelli DJ. 1999. Tool use, aye-ayes, and sensorimotor intelligence. Folia Primatol (Basel) 70:8–16.

Sundgren PC, Dong Q, Gómez-Hassan D, Mukherji SK, Maly P, Welsh R. 2004. Diffusion tensor imaging of the brain: review of clinical applications. Neuroradiology 46:339–350.

Tattersall I. 1982. The primates of Madagascar. New York: Columbia University Press.

Yoder AD. 1994. Relative position of the cheirogaleidae in strepsirhine phylogeny: a comparison of morphological and molecular methods and results. Am J Phys Anthropol 94:25–46.

Yoder AD, Yang Z. 2004. Divergence dates for Malagasy lemurs estimated from multiple gene loci: geological and evolutionary context. Mol Ecol 13:757–773.

Zhang S, Demiralp C, Laidlaw DH. 2003. Visualizing diffusion tensor MR images using streamtubes and streamsurfaces. IEEE T Vis Comput Gr 9:454–462.

Ziehen T. 1896. Ueber die Grosshirnfurchung der Halbaffen und die Deutungeiniger Furchen des menschliched Gehirns. Arch Psyciat Nervenkr 28:898–930.